Contribution from the Departments of Chemistry, Texas A&M University, College Station, Texas 77843, and University of Delaware, Newark, Delaware 19716

Comparative Reactivities of Anionic Group 6 Alkyl, Silyl, and Stannyl Pentacarbonyl Metalates toward Carbon Dioxide and Sulfur Dioxide. Crystal Structure of $[PPN][W(CO)_5Si(CH_3)_3]$

Donald J. Darensbourg,*[1a] Christopher G. Bauch,[1a] Joseph H. Reibenspies,[1a] and Arnold L. Rheingold[1b]

Received April 19, 1988

The syntheses of $[PPN][M(CO)_5SiR_3]$ (M = Cr, R = CH_3; M = W, R = CH_3, C_2H_5) and $[PPN][W(CO)_5SnR_3]$ (R = CH_3, C_6H_5) from the reactions of $Na_2M(CO)_5$ and the corresponding R_3SiCl or R_3SnCl reagents are reported. The complex $[PPN][W(CO)_5Si(CH_3)_3]$ has been characterized in the solid state via X-ray crystallography. $[PPN][W(CO)_5Si(CH_3)_3]$ crystallizes in the space group $P\bar{1}$, with cell dimensions a = 10.664 (2) Å, b = 12.739 (4) Å, c = 5.75 Å, α = 97.75 (2)°, β = 92.18 (2)°, γ = 96.13 (2)°, V = 2105.0 (9) Å^3, Z = 2, and R_F = 4.12%. Comparisons of the $(CO)_5W$–group 14 element bond lengths reveal the W–Si and W–Sn bonds to be shorter than that which would be anticipated on the basis of the sum of the single-bond covalent radii. This bond shortening is ascribed to d_π–d_π back-bonding from the metal to Si or Sn. Consistent with a stronger W–Si and W–Sn bond as compared with that for the carbon analogue $[W(CO)_5CH_3]^-$, unlike the alkyl species, these silyl and stannyl derivatives were found to be inert toward CO_2, even when dissolved in pure carbon dioxide at 800 psi. On the other hand, all $(CO)_5W$–group 14 element bonds readily undergo reactions with the more electrophilic sulfur dioxide to provide the corresponding sulfinate-*S* complexes. For example, $[(CO)_5W\text{–}Sn(CH_3)_3]^-$ reacts instantaneously at ambient temperature with SO_2 to eventually yield $[(CO)_5W\text{–}S(O)_2Sn(CH_3)_3]^-$. In this instance infrared and NMR spectral evidence for the intermediacy of the sulfinate-*O* complex is found. In a subsequent process this complex isomerizes to the thermodynamically more stable sulfinate-*S* derivative.

The insertion of carbon dioxide into metal–carbon bonds is a pivotal step in carbon homologation processes involving carbon dioxide.[2] Thus, this insertion reaction (eq 1) is of great interest

$$M\text{—}R + CO_2 \longrightarrow M\text{—}O\text{—}\overset{\overset{O}{\|}}{C}\text{—}R \qquad (1)$$

for the utilization of carbon dioxide as a source of chemical carbon. The carbon–carbon bond-forming process has been shown to proceed via an I_a mechanism with retention of configuration about the α-carbon atom of the alkyl group.[3] On the other hand, insertion of the more electrophilic sulfur dioxide molecule into metal–carbon bonds has been demonstrated to occur by an S_E2 mechanism with SO_2 attacking at the back side of the alkyl group to initially afford the sulfinate-*O* complex, with subsequent rearrangement to the sulfinate-*S* product (eq 2).[4]

$$M\text{—}R + SO_2 \longrightarrow [M^+O_2SR^-] \longrightarrow M\text{—}\overset{\overset{O}{\|}}{\underset{\underset{O}{\|}}{S}}\text{—}R \qquad (2)$$

The anionic group 6 metal alkyl and aryl complexes readily react with either carbon monoxide or carbon dioxide to provide the corresponding acyl- or carboxylate–metal derivatives. Hence, it is anticipated that sulfur dioxide should undergo insertion into these metal–carbon bonds in a very facile manner. This latter process is reported upon herein for reactions involving $RW(CO)_5^-$ (R = Ph, Me) derivatives. Furthermore, we have extended our studies of CO_2 or SO_2 insertion processes to include complexes containing tungsten bonded to other group 14 elements, namely silicon and tin. In this regard the present article reports the synthesis and structures of the complexes $[M(CO)_5M'R_3]^-$ (M = Cr, W; M′ = Si, Sn; R = Me, Et, Ph). Comparative reactivity investigations of these species with their carbon analogues are presented. Of particular interest are their reactions with the unsaturated substrates CO_2 and SO_2. In part our reason for extending our studies to include the silyl derivatives was that we felt that these species should represent the best cases for observing *abnormal* CO_2 insertion reactions (eq 3) because of the strength

$$[M]\text{—}SiR_3 + CO_2 \longrightarrow [M]\text{—}\overset{\overset{O}{\|}}{C}\text{—}OSiR_3 \qquad (3)$$

of the Si–O bond. During the course of these studies we have structurally characterized the $[PPN][W(CO)_5Si(CH_3)_3]$ salt by X-ray crystallography.

Experimental Section

Methods and Materials. All manipulations were carried out either in an argon drybox or on a double-manifold Schlenk vacuum line, using freshly distilled solvents. Reagent grade tetrahydrofuran and hexane were purified by distillation under nitrogen from sodium benzophenone ketyl. Diethyl ether was refluxed under nitrogen over lithium aluminum hydride before use. $W(CO)_6$ and bis(triphenylphosphine)nitrogen(1+) chloride ([PPN][Cl]) were purchased from Strem Chemicals Inc. Triethylsilyl chloride, trimethylsilyl chloride, and trimethyltin chloride were obtained from Aldrich Chemical Co. Carbon dioxide and sulfur dioxide were provided by Airco.

Infrared spectra were recorded on a Perkin-Elmer 283B, and IBM FTIR/85, or an IBM FTIR 32 spectrometer. Proton, ^{13}C, and ^{119}Sn NMR spectra were determined on either a Varian XL-200 or a Varian XL-400 spectrometer.

Preparations. $[PPN][W(CO)_5SO_2R]$ (R = CH_3, C_6H_5). In a typical reaction, the alkyl or aryl complex (ca. 0.1 mmol; 0.088 g $[PPN][W(CO)_5CH_3]$,[5] 0.094 g $[PPN][W(CO)_5C_6H_5]$[5]) was loaded into a 100-mL Schlenk flask, which was evacuated and backfilled with nitrogen. After addition of 30 mL of THF, the flask was evacuated and refilled with sulfur dioxide gas to atmospheric pressure. Infrared spectroscopy indicated complete conversion to the sulfinate upon mixing. The solvent was reduced in volume by half in vacuo, and the product, upon addition of hexane, was isolated as a yellow solid product. ^1H NMR (where R = CH_3; in $(CD_3)_2CO$): δ 2.74 (s, 3 H), 7.72 ppm (m, 30 H). The infrared bands of the carbonyl stretching frequencies in THF are as follows (cm^{-1}): $[PPN][W(CO)_5SO_2CH_3]$, 1901 (m), 1934 (s), 2072 (w); $[PPN][W(CO)_5SO_2C_6H_5]$, 1891 (m), 1930 (s), 2067 (w).

$[PPN][M(CO)_5SiR_3]$ (M = Cr, W; R = CH_3, C_2H_5). In a typical preparation a solution of $W(CO)_5NMe_3$[6] (0.484 g, 1.26 mmol) in 30 mL of THF cooled to −78 °C was titrated with sodium naphthalenide (0.14 M in THF) until the green color persisted, generating $Na_2W(CO)_5$. Trimethylsilyl chloride (0.23 mL, 1.80 mmol) was added and the solution

(1) (a) Texas A&M University. (b) University of Delaware.
(2) (a) Eisenberg, R.; Henderiksen, D. E. *Adv. Catal.* **1979**, *28*, 79. (b) Vol'pin, M. E.; Kolomnikov, I. S. *Pure Appl. Chem.* **1973**, *33*, 567. (c) Ito, T.; Yamamoto, A. In *Organic and Bioinorganic Chemistry of Carbon Dioxide*; Inoue, S., Yamazaki, N., Eds.; Kodansha: Tokyo, 1982; p 79. (d) Sneeden, R. P. A. In *Comprehensive Organometallic Chemistry*; Wilkinson, G., Stone, F. G. A., Abel, E. W., Eds.; Pergamon: Oxford, U.K., 1982; Vol. 8, p 225. (e) Darensbourg, D. J.; Kudarowski, R. *Adv. Organomet. Chem.* **1983**, *22*, 129. (f) Palmer, D. A.; van Eldik, R. *Chem. Rev.* **1983**, *83*, 651. (g) Walther, D. *Coord. Chem. Rev.* **1987**, *79*, 135. (h) Braunstein, P.; Matt, D.; Nobel, D. *Chem. Rev.*, in press.
(3) (a) Darensbourg, D. J.; Hanckel, R. K.; Bauch, C. G.; Pala, M.; Simmons, D.; White, J. N. *J. Am. Chem. Soc.* **1985**, *107*, 7463. (b) Darensbourg, D. J.; Grötsch, G. *J. Am. Chem. Soc.* **1985**, *107*, 7473.
(4) (a) Whitesides, G. M.; Boschetto, D. J. *J. Am. Chem. Soc.* **1971**, *93*, 1529. (b) Wojcicki, A. *Adv. Organomet. Chem.* **1974**, *12*, 31. (c) Jacobsen, S. E.; Wojcicki, A. *J. Am. Chem. Soc.* **1973**, *95*, 692.
(5) Alcock, N. W. *Acta Crystallogr.* **1974**, *A30*, 332.
(6) Darensbourg, D. J.; Bauch, C. G.; Rheingold, A. L. *Inorg. Chem.* **1987**, *26*, 977.

0020-1669/88/1327-4203$01.50/0

Table I. Crystallographic Data for $[PPN][W(CO)_5Si(CH_3)_3]$

mol formula	$C_{44}H_{39}NO_5P_2SiW$	V, Å^3	2105.0 (9)
space group	$P\bar{1}$	Z	2
a, Å	10.664 (2)	D(calcd), g/cm^3	1.482
b, Å	12.739 (4)	μ(Mo Kα), cm^{-1}	30.5
c, Å	5.75	wavelength, Å	0.710 73
α, deg	97.75 (2)	R_F, %[a]	4.12
β, deg	92.18 (2)	R_{wF}, %[a]	4.39
γ, deg	96.13 (2)		

[a] $R_F = \sum|\Delta|/\sum|F_o|$ and $R_{wF} = \sum(|\Delta|w^{1/2})/\sum(|F_o|w^{1/2})$, where $\Delta = |F_o| - |F_c|$.

allowed to warm slowly to room temperature. After the addition of [PPN][Cl] (0.72 g, 1.26 mmol), the solution was stirred for 15 min and then filtered through Celite. The filtrate volume was reduced to half the original quantity under reduced pressure, and the product was precipitated upon addition of 30 mL of hexane.

For R = CH_3 and M = W, the product was purified by recrystallization from THF/hexane. Crystals were grown from THF/Et_2O/hexane (1:1:1) at −20 °C. Recrystallization was performed from Et_2O/hexane for the complex with R = C_2H_5 and M = W. The infrared spectra in the carbonyl region, with THF as solvent, are as follows (cm^{-1}): $[PPN][W(CO)_5Si(CH_3)_3]$, 1865 (m), 1885 (s), 2020 (w); $[PPN][W(CO)_5Si(C_2H_5)_3]$, 1864 (m), 1885 (s), 2020 (w); $[PPN][Cr(CO)_5Si(CH_3)_3]$, 1865 (sh), 1878 (s), 2005 (w). Anal. Calcd for $[PPN][W(CO)_5Si(CH_3)_3]$: C, 56.48; H, 4.20; N, 1.50; P, 6.62. Found: C, 56.21; H, 4.25; N, 1.43; P, 6.54.

$[PPN][W(CO)_5SnR_3]$ (R = CH_3, C_6H_5). These complexes were synthesized in a manner completely analogous to that for $[PPN][W(CO)_5Si(CH_3)_3]$ with R_3SnCl as the electrophile. X-ray-quality crystals of $[PPN][W(CO)_5Sn(CH_3)_3]$ were grown from THF/Et_2O/hexane (1:1:1). The carbonyl stretching frequencies, in THF solvent, are as follows (cm^{-1}): $[PPN][W(CO)_5Sn(CH_3)_3]$, 1868 (m), 1891 (s), 2023 (w); $[PPN][W(CO)_5Sn(C_6H_5)_3]$, 1879 (m), 1904 (s), 2035 (w). Anal. Calcd for $[PPN][W(CO)_5Sn(CH_3)_3]$: C, 51.49; H, 3.83; N, 1.46; P, 6.04. Found: C, 51.25; H, 3.72; N. 1.38; P, 5.98.

$[PPN][W(CO)_5SO_2M'R_3]$ ($M'R_3$ = $Si(CH_3)_3$, $Sn(C_6H_5)_3$). In a typical reaction, $[PPN][W(CO)_5Sn(CH_3)_3]$ (0.1 g) was loaded into a 100-mL Schlenk flask, which was evacuated and backfilled with nitrogen. After addition of 30 mL of THF, the flask was evacuated and refilled with sulfur dioxide gas to atmospheric pressure. Infrared spectroscopy indicated complete conversion to the sulfinate after ca. 10 min. The solvent was reduced in volume by half in vacuo, and the product was precipitated as a yellow solid product upon addition of hexane.

When the above reaction was performed at −78 °C, it was possible to observe the formation of the sulfinate-*O* species in the infrared spectrum. For $M'R_3 = Sn(C_6H_5)_3$, the reaction required 30 min to go to completion. A 2-h reaction time was required to fully convert the silyl complex ($M'R_3$ = $Si(CH_3)_3$) to the inserted product. The infrared spectra in the ν(CO) region in THF solvent are as follows (cm^{-1}): $[PPN][W(CO)_5SO_2Sn(CH_3)_3]$, 1901 (m), 1934 (s), 2072 (w); $[PPN][W(CO)_5OS(O)Sn(CH_3)_3]$, 1895 (m), 1911 (s), 2043 (w); $[PPN][W(CO)_5SO_2Sn(C_6H_5)_3]$, 1906 (m), 1935 (s), 2062 (w); $[PPN][W(CO)_5SO_2Si(CH_3)_3]$, 1871 (m), 1935 (s), 2058 (w).

Crystallographic Studies. $[PPN][W(CO)_5Si(CH_3)_3]$. A crystal of $C_{44}H_{39}NOP_2SiW$ was attached to a fine glass fiber with epoxy cement. The compound crystallizes in the triclinic space group $P\bar{1}$ with $Z = 2$. Parameters for the collection and refinement of the crystallographic data are contained in Tables I and 1S (Table 1S is given in the supplementary material). Unit cell dimensions were derived from the least-squares fit of the angular settings of 25 reflections with $19° \leq 2\theta \leq 25°$.

The structure was solved via heavy-atom methods. The remaining non-hydrogen atoms were located from subsequent difference Fourier syntheses. All non-hydrogen atoms were refined anisotropically. Hydrogen atoms were calculated and fixed in idealized positions: d(C–H) = 0.96 Å; U = 1.2 times U_{iso} for the carbon to which it was attached. The cation phenyl rings were constrained to rigid hexagons to conserve data. Data were corrected for absorption effects by an empirical procedure that employs six refined parameters to define a pseudoellipsoid used to calculate corrections. An inspection of F_o vs F_c values and trends based upon sin θ and Miller index parity group failed to reveal any systemic errors in the data. All computer programs used in the data collection and refinement are contained in the Nicolet (Madison, WI) program packages P3 and SHELXTL (version 5.1).

Results

Synthesis. The silyl and stannyl tungsten and chromium pentacarbonyl metalates were synthesized by the reaction of the pentacarbonyl dianion with the appropriate trialkylsilyl or -stannyl chloride. This synthetic method is completely analogous to the procedure we have previously described for the production of the alkyl complexes.[6] Ellis and co-workers have reported[7] the synthesis of the triphenyltin complexes $[Et_4N][Ph_3SnM(CO)_5]$ (where M = Cr, Mo, W), as a means of derivatizing $M(CO)_5^{2-}$. In addition to a novel route to the tungsten derivative has recently been described as resulting from the reaction of Ph_3SnOH and $HW(CO)_5^-$ (eq 4).[8] An alternate method for the synthesis of a variety

$$PH_3SnOH + [PPN][HW(CO)_5] \rightarrow H_2O + [PPN][Ph_3SnW(CO)_5] \quad (4)$$

of trialkyl group 14–group 6 pentacarbonyl anions has been reported by Isaacs and Graham.[9] The reaction of $R_3M'Li$ with $[Et_4N][M(CO)_5Cl]$ was employed to produce a number of complexes, where R_3M' = Ph_3Si, $MePh_2Si$, Ph_3Ge, Ph_3Sn, Me_3Sn, and Ph_3Pb.

The silyl and stannyl complexes reported upon herein proved to be rather unreactive to a variety of substrates. Among these were CO_2 (500 psi, 150 °C), CS_2 (THF solution, 40 °C, 48 h), benzaldehyde (neat solution, 23 °C, 48 h), water (THF solution, 23 °C, 48 h), and methanol (neat solution, 23 °C, 48 h). A THF solution of $[PPN][W(CO)_5Si(CH_3)_3]$ also did not react with acetic acid. However, addition of an equimolar amount of concentrated hydrochloric acid led to the immediate formation of $[PPN][W(CO)_5Cl]$ and presumably $(CH_3)_3SiH$. On the other hand, these derivatives readily reacted with SO_2 to eventually afford sulfinate-*S* derivatives.

Results and Discussion of the Structure of $[PPN][W(CO)_5Si(CH_3)_3]$. The final atomic coordinates for all non-hydrogen atoms of the anion are provided in Table II. Bond lengths and angles for the $[W(CO)_5Si(CH_3)_3]^-$ unit are shown in Tables III and IV. The structure of the complex consists of an array of two discrete ionic units at normal van der Waals distances. Figure 1 dipicts the three-dimensional structure of the anion.

The ligands are distributed in a distorted-octahedral relationship around the tungsten atom with an average OC(C(1))–W–CO(eq)

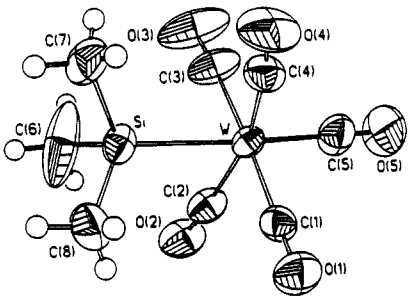

Figure 1. ORTEP plot and labeling scheme for the anion $W(CO)_5Si(CH_3)_3^-$.

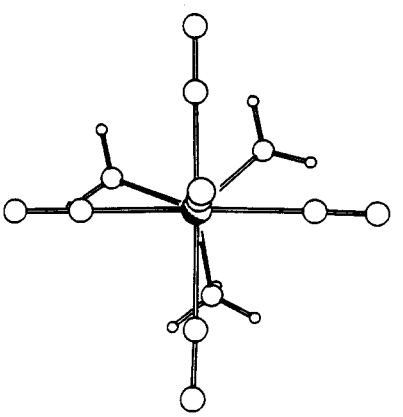

Figure 2. Perspective view of the anion $W(CO)_5Si(CH_3)_3^-$.

(7) Ellis, J. P.; Hentges, S. G.; Kalina, D. G.; Hagen, G. P. *J. Organomet. Chem.* **1975**, *97*, 79.
(8) Darensbourg, M. Y.; Liaw, W.-F.; Reibenspies, J. *Inorg. Chem.* **1988**, *27*, 2555.
(9) Isaacs, E. E.; Graham, W. A. G. *Can. J. Chem.* **1975**, *53*, 467.

Table II. Atomic Coordinates ($\times 10^4$) and Isotropic Thermal Parameters ($Å^2 \times 10^3$)

	x	y	z	U[a]
W	896.6 (2)	929.2 (2)	2191.5 (2)	51.2 (1)
Si	2279 (2)	1215 (2)	3628 (1)	63 (1)
O(1)	3007 (6)	−190 (5)	1188 (4)	99 (3)
O(2)	46 (6)	−1193 (4)	2947 (4)	102 (3)
O(3)	−1001 (7)	2125 (6)	3341 (6)	164 (4)
O(4)	2437 (7)	3147 (5)	2039 (5)	119 (3)
O(5)	−980 (8)	656 (7)	565 (5)	153 (4)
C(1)	2230 (6)	201 (6)	1554 (4)	62 (3)
C(2)	307 (7)	−446 (6)	2647 (5)	72 (3)
C(3)	−329 (8)	1699 (7)	2912 (7)	94 (4)
C(4)	1836 (8)	2325 (6)	2055 (5)	73 (3)
C(5)	−291 (8)	758 (8)	1163 (5)	91 (4)
C(6)	1404 (13)	779 (11)	4540 (6)	193 (8)
C(7)	2932 (9)	2645 (7)	4025 (5)	94 (4)
C(8)	3715 (11)	474 (8)	3614 (7)	138 (6)
N	5530 (4)	5681 (4)	2734 (3)	39 (2)
P(1)	6704 (1)	5399 (1)	2200 (1)	34 (1)
P(2)	4673 (1)	6632 (1)	2865 (1)	37 (1)
C(11)	5631 (4)	3308 (3)	2049 (2)	52 (2)
C(12)	5473	2238	1686	75 (3)
C(13)	6096	1909	950	78 (3)
C(14)	6877	2649	578	77 (3)
C(15)	7035	3719	941	59 (2)
C(16)	6412	4049	1676	41 (2)
C(21)	6226 (3)	6130 (3)	666 (2)	47 (2)
C(22)	6422	6822	56	56 (2)
C(23)	7443	7618	169	62 (3)
C(24)	8268	7722	892	59 (2)
C(25)	8073	7031	1501	45 (2)
C(26)	7052	6235	1388	35 (2)
C(31)	9031 (4)	4803 (4)	2670 (3)	74 (3)
C(32)	10145	4903	3182	93 (4)
C(33)	10333	5673	3908	94 (4)
C(34)	9406	6343	4121	109 (4)
C(35)	8292	6243	3609	80 (3)
C(36)	8105	5474	2883	40 (2)
C(41)	5306 (4)	8306 (3)	1956 (2)	52 (2)
C(42)	6000	9254	1819	72 (3)
C(43)	6836	9820	2465	78 (3)
C(44)	6977	9473	3248	78 (3)
C(45)	6283	8489	3385	61 (2)
C(46)	5448	7923	2739	42 (2)
C(51)	3706 (4)	7612 (3)	4352 (3)	69 (3)
C(52)	3198	7606	5155	79 (3)
C(53)	3098	6674	5534	72 (3)
C(54)	3507	5748	5110	66 (3)
C(55)	4015	5754	4308	52 (2)
C(56)	4115	6686	3929	41 (2)
C(61)	3013 (3)	5417 (3)	1629 (3)	47 (2)
C(62)	1932	5231	1080	60 (2)
C(63)	1136	6027	1048	63 (3)
C(64)	1422	7009	1564	71 (3)
C(65)	2503	7196	2114	58 (2)
C(66)	3299	6399	2146	40 (2)

[a] Equivalent isotropic U defined as one-third of the trace of the orthogonalized U_{ij} tensor.

Table III. Bond Lengths (Å) for $[PPN][W(CO)_5Si(CH_3)_3]$

W–Si	2.614 (2)	O(3)–C(3)	1.134 (13)
W–C(1)	2.007 (7)	O(4)–C(4)	1.171 (10)
W–C(2)	2.029 (2)	O(5)–C(5)	1.157 (11)
W–X(3)	2.011 (9)	N–P(1)	1.580 (5)
W–C(4)	1.988 (8)	N–P(2)	1.591 (5)
W–C(5)	1.991 (8)	P(1)–C(16)	1.794 (4)
Si–C(6)	1.857 (12)	P(1)–C(26)	1.796 (4)
Si–C(7)	1.892 (8)	P(1)–C(36)	1.794 (5)
Si–C(8)	1.882 (12)	P(2)–C(46)	1.799 (4)
O(1)–C(1)	1.146 (9)	P(2)–C(56)	1.794 (5)
O(2)–C(2)	1.132 (10)	P(2)–C(66)	1.791 (4)

angle of 95.4°. Three of the equatorial CO ligands (C(2)–C(4)) are bent toward the trimethylsilyl group, with an average OC–W–Si bond angle of 82.2°. The remaining equatorial ligand shows an angle of this type nearly 10° larger than the other three. A reason for this may be the orientation of the methyl groups of the silicon atom. In Figure 2, which shows the anion down the O(5), C(5), W, Si axis, C(8) can be seen to be in a nearly eclipsed arrangement relative to C(1) while the other methyl groups are staggered with respect to the carbonyl ligands.

Table IV. Bond Angles (deg) for $[PPN][W(CO)_5Si(CH_3)_3]$

Si–W–C(1)	91.7 (2)	C(6)–Si–C(8)	103.9 (6)
Si–W–C(2)	80.6 (2)	C(7)–Si–C(8)	103.7 (4)
C(1)–W–C(2)	90.0 (3)	W–C(1)–O(1)	178.3 (6)
Si–W–C(3)	83.6 (3)	W–C(2)–O(2)	174.9 (7)
C(1)–W–C(3)	175.2 (3)	W–C(3)–O(3)	177.7 (9)
C(2)–W–C(3)	90.4 (3)	W–C(4)–O(4)	174.6 (7)
Si–W–C(4)	82.1 (2)	W–C(5)–O(5)	179.8 (8)
C(1)–W–C(4)	88.8 (3)	P(1)–C(16)–C(11)	119.3 (1)
C(2)–W–C(4)	162.6 (3)	P(1)–C(16)–C(15)	120.5 (1)
C(3)–W–C(4)	89.5 (3)	P(1)–C(26)–C(21)	118.8 (1)
Si–W–C(5)	174.5 (3)	P(1)–C(26)–C(25)	121.1 (1)
C(1)–W–C(5)	93.7 (3)	P(1)–C(36)–C(31)	120.4 (1)
C(2)–W–C(5)	98.6 (3)	P(1)–C(36)–C(35)	119.5 (1)
C(3)–W–C(5)	91.0 (4)	P(2)–C(46)–C(41)	119.3 (1)
C(4)–W–C(5)	98.9 (4)	P(2)–C(46)–C(45)	120.3 (1)
W–Si–C(6)	113.0 (4)	P(2)–C(56)–C(51)	121.4 (1)
W–Si–C(7)	115.3 (3)	P(2)–C(56)–C(55)	118.4 (1)
C(6)–Si–C(7)	104.2 (5)	P(2)–C(66)–C(61)	120.1 (1)
W–Si–C(8)	115.4 (3)	P(2)–C(66)–C(65)	119.9 (1)

Table V. Bond Lengths in Anionic Tungsten Derivatives

bond type	bond dist, Å	diff, Å[a]
$(CO)_5W–CH_3^-$	2.313 (17)[b]	1.543
$(CO)_5W–Si(CH_3)_3^-$	2.614 (2)[c]	1.444
$(CO)_5W–Sn(CH_3)_3^-$	2.810 (8)[c]	1.410

[a] Covalent radii for C(sp^3), Si, and Sn of 0.77, 1.17, and 1.40 Å, respectively, were those reported by Cotton, F. A.; Wilkinson, G.; Gaus, P. L. *Basic Inorganic Chemistry*, 2nd ed., Wiley: New York, 1987; p 93. [b] Taken from ref 5. [c] This work.

The average W–CO(eq) bond distance of 2.008 Å is 0.087 Å longer than the axial W–CO bond length at 1.92 Å. This trans effect is typical of anionic tungsten pentacarbonyl complexes such as $[W(CO)_5O_2CCH_3]^-$, which demonstrates[10] the same axial W–CO bond shortening as seen here in the trimethylsilyl complex. The W–Si bond length is 2.614 Å.

A similar structure determination on the $[PPN][W(CO)_5Sn(CH_3)_3]$ salt was attempted.[11] The crystal displayed two complete anion–cation pairs per unit cell with one of the anionic units being disordered. The disorder was caused by two superimposed metal anions. Each anion shared the W metal and two carbonyl ligands in common. The position of the Sn atom and the remaining carbonyls was disordered between two positions. Four carbonyl ligand atoms and the Sn atom were included for one position; however, only the location of the Sn atom could be determined for the second position. The most useful metric information derived for the anion is the W–Sn distance of 2.810 (8) Å, which is similar to that determined for the W–Sn bond distance in the $[W(CO)_5SnPh_3]^-$ anion (2.812 (1) Å).[8]

Discussion

Comparisons of $(CO)_5W$–Group 14 Element Bonds. Because of the comparative reactivity studies to be discussed later, i.e., CO_2 insertion processes involving the W–group 14 element bond, it is worthwhile to examine the differences in bond distances observed in these derivatives. We have previously reported the X-ray structure of $[Na(18\text{-crown-}6)][W(CO)_5CH_3]$ at −88 °C

(10) Cotton, F. A.; Darensbourg, D. J.; Kolthammer, B. W. S.; Kudaroski, R. *Inorg. Chem.* **1982**, *21*, 1656.

(11) The $[PPN][W(CO)_5Sn(CH_3)_3]$ salt crystallized as two independent cation–anion pairs located in the asymmetric unit in the space group $P2_1/n$. Intensity data were collected in a Nicolet R3m/V diffractometer utilizing graphite-monochromated molybdenum Kα radiation (λ = 0.71073 Å) at a temperature of 20 ± 1 °C. A total of 2663 unique reflections were collected. Crystal data for $[PPN][W(CO)_5Sn(CH_3)_3]$: $C_{44}H_{39}NO_5P_2SnW$, M_r = 1026.3, monoclinic, a = 16.347 (5) Å, b = 19.098 (6) Å, c = 7.911 (9) Å, β = 85.01 (3)°, V = 8680 (5) Å^3, Z = 8, μ = 33.1 cm^{-1}.

Table VI. Carbonyl Stretching Frequencies (cm^{-1}) and Force Constants (mdyn/Å) for $W(CO)_5X^-$ Derivatives[a]

X	ν_{CO}			force const[b]		
	$A_1^{(2)}$	$A_1^{(1)}$	E	k_1	k_2	k_c
CH_3	2030	1836	1883	13.79	15.04	0.359
$Si(CH_3)_3$	2020	1865	1885	14.25	15.00	0.324
$Sn(CH_3)_3$	2023	1868	1891	14.28	15.09	0.316
Cl	2062	1846	1914	13.94	15.53	0.370

[a] Frequencies measured in tetrahydrofuran solvent. [b] Force constant definitions may be found in ref 14.

and found the W–CH_3 bond distance to be 2.313 (17) Å.[6] Unfortunately, we have not been able to obtain crystals of $[W(CO)_5C(CH_3)_3]^-$ for a similar measurement; however, the W–C bond distance is not expected to be significantly diffferent in these species. Table V lists the relevant bond lengths for $(CO)_5W$–group 14 element derivatives, along with the difference between these bond distances and the single-bond covalent radii of the group 14 elements.

It is evident from the bond lengths given in Table V that the W–Si and W–Sn bond distances are less than would be anticipated on the basis of the sum of the single-bond covalent radii, assuming the single-bond covalent radius of tungsten is that noted in the methyl complex (1.54 Å). A similar value (1.55 Å) for the sinlge-bond radius of tungsten can be calculated from the W–Cl bond length measured in $[(CO)_5W\text{–}Cl]^-$ of 2.54 (1) Å and the single-bond covalent radius of chlorine of 0.99 Å.[12] This bond shortening for Si and Sn is ascribable to d_π–d_π back-bonding from the metal to the group 14 element.[13]

Further, it is of interest to compare the nature of the bonding in these species as inferred from ν(CO) vibrational spectroscopy. Provided in Table VI are the CO stretching frequencies and force constants for these complexes,[14] as well as those for $[(CO)_5WCl]^-$. The stretching force constants for the cis carbonyl ligands in the group 14 complexes are all quite similar, ranging from 15.00 to 15.09 mdyn/Å. On the other hand, force constant for the carbonyl ligand trans to the methyl ligand is significantly lower (~0.5 mdyn/Å) than the corresponding values for the $-Si(CH_3)_3$ and $-Sn(CH_3)_3$ complexes. That is, the Si and Sn analogues can be inferred to be better π-acceptors. Consistent with these arguments, the Cl ligand displays a large separation in k_1 and k_2.

Insertion Reactions. Carbon Dioxide Insertion. Despite the affinity the $[M(CO)_5R]^-$ derivatives display toward carbon dioxide as evidenced by insertion reactions such as shown in eq 5, the silyl and stannyl complexes were found to be unreactive toward CO_2.

$$[(CO)_5W\text{—}CH_3]^- + CO_2 \longrightarrow [(CO)_5W\text{—}O\text{—}\overset{\overset{O}{\|}}{C}\text{—}CH_3]^- \quad (5)$$

Unsuccessful reactions were performed in THF at CO_2 pressures in excess of 1000 psi or in pure carbon dioxide at 800 psi.[15] This lack of reactivity is most likely due to the strength of the W–Si and W–Sn bonds (vide supra). Insertion of benzaldehyde into the W–Si bond, a process that has been reported for $Mn(CO)_5Si(CH_3)_3$ (eq 6),[16] did not occur in the case of $[(CO)_5WSi(CH_3)_3]^-$.

$$(CO)_5MnSi(CH_3)_3 + HC(O)C_6H_5 \longrightarrow (CO)_5Mn\text{—}\overset{\overset{OSi(CH_3)_3}{|}}{\underset{\underset{H}{|}}{C}}\text{—}C_6H_5 \quad (6)$$

Sulfur Dioxide Insertion. The insertion of sulfur dioxide into the metal–carbon bond of $[W(CO)_5R]^-$ (R = CH_3, C_6H_5) complexes occurs much more readily than the insertion of carbon dioxide or carbon monoxide. The reaction is complete upon admission of SO_2 gas to a THF solution of the alkyl complex at ambient temperature. The infrared spectrum of the product of the reaction of SO_2 and $[PPN][W(CO)_5C_6H_5]$ exhibited carbonyl stretching frequencies similar to those reported by Wojcicki and co-workers for $Na[W(CO)_5SO_2C_6H_5]\cdot 2CH_3OH$.[17] This complex was prepared by the reaction of $C_6H_5SO_2Na$ and $[(n\text{-}C_4H_9)_4N][W(CO)_5I]$. The nature of the metal–sulfinate attachment in the product was determined to be that of a sulfur-bonded sulfinate by analysis of the asymmetric and symmetric S–O stretching frequencies. These occur in the ranges 1112–1100 and 1050–1000 cm^{-1}, respectively. Sulfur–oxygen stretches above 1000 cm^{-1} are found in sulfinate-*S* species while S–O stretching frequencies below 1000 cm^{-1} are indicative of complexes with M–OS(O)R bonds.[18,19] Similar S–O stretching frequencies were found in the products formed by the SO_2 insertion reaction with $[PPN][W(CO)_5C_6H_5]$. The S–O stretching frequencies were seen at 1131, 1075, 1025, and 1016 cm^{-1} (in mineral oil mull).

The anionic alkyl tungsten complexes were found to be much more reactive than the isoelectronic neutral rhenium analogues. $Re(CO)_5CH_3$ was reported to undergo insertion only after refluxing in liquid SO_2 for 6 h,[17] while $[W(CO)_5CH_3]^-$ inserted SO_2 immediately upon addition of the gas to a THF solution. The increase in rate can be attributed to the higher electron density present in the anionic complex. Other studies have reported that the replacement of an ancillary carbonyl ligand by a more basic ligand enhances the rate of SO_2 insertion into a metal alkyl. For example, $CpFe(CO)(PPh_3)CH_2Ph$ reacts rapidly with SO_2 in chloroform solution,[20] while the parent $CpFe(CO)_2CH_2Ph$ species is unreactive under comparable conditions. The rate enhancement is likely to be even more greatly affected by the presence of a negatively charged species than the increase in ligand basicity. However, there have been no reported instances of SO_2 insertion for any other anionic metal alkyl complexes.

Similar rate enhancement effects have been noted for CO_2 insertion.[3] However, the greater electrophilicity of SO_2 allows for insertion into the metal–carbon bonds of alkyl complexes that are unreactive toward CO_2 insertion (e.g. $CH_3Re(CO)_5$). The insertion of CO_2 is mechanistically different from that of SO_2. While CO_2 has been demonstrated to insert via an associative-interchange mechanism with retention of configuration at carbon,[3b] SO_2 is generally believed[4b] to insert by an S_E2 type mechanism with back-side attack at the alkyl carbon causing an inversion of configuration. Both insertions are electrophilic in nature; however, the position of initial interaction differs. For CO_2 insertion, primary attack occurs at the metal center, while for SO_2, sulfur first interacts with the alkyl carbon whereupon it subsequently rearranges to form the sulfinate product.

Although the silyl and stannyl anionic tungsten(0) derivatives are completely inert toward carbon dioxide, these species readily react with the more electrophilic sulfur dioxide molecule. For example, the addition of 1 atm of SO_2 pressure to a THF solution of $[PPN][W(CO)_5Sn(CH_3)_3]$ at ambient temperature led to an immediate color change from colorless to light yellow. An infrared spectrum taken immediately upon addition of SO_2 demonstrated the complete disappearance of the starting material carbonyl frequencies and the presence of new bands at 1912 (s), 1930 (s), 2043 (sh), and 2059 (w) cm^{-1}. When the mixture is stirred for 10 min, the peaks at 1912 and 2043 cm^{-1} had disappeared, leaving behind bands at 1914 (sh), 1930 (s), and 2059 (w) cm^{-1}. This pattern denotes that the product is an $[M(CO)_5X]^-$ species with IR bands of symmetry E + 2 A_1. The spectrum is closely related to that of the alkane sulfinates, which have been unambiguously determined to be sulfur-bonded sulfinate complexes. In order to identify the transient species observed in the room-temperature infrared spectrum, the reaction was performed at reduced tem-

(12) (a) Burschka, Ch.; Schenk, W. A. *Z. Anorg. Allg. Chem.* **1981**, *477*, 149. (b) Darensbourg, D. J.; Bauch, C. G., unpublished observations.
(13) Cundy, C. S.; Kingston, B. M.; Lappert, M. F. *Adv. Organomet. Chem.* **1971**, *2*, 253.
(14) Cotton, F. A.; Kraihanzel, C. S. *J. Am. Chem. Soc.* **1962**, *84*, 4432.
(15) $[PPN][W(CO)_5M(CH_3)_3]$ complexes, where M = Si, Sn, were shown to be completely soluble in pure liquid carbon dioxide.
(16) Johnson, D. L.; Gladysz, J. A. *Inorg. Chem.* **1981**, *20*, 2508.
(17) Hartman, F. A.; Wojcicki, A. *Inorg. Chem.* **1968**, *7*, 1504.
(18) Deacon, G. B.; Felder, P. W. *J. Am. Chem. Soc.* **1968**, *90*, 493.
(19) Langs, D. A.; Hare, C. R. *Chem. Commun.* **1967**, 853.
(20) Graziani, M.; Wojcicki, A. *Inorg. Chim. Acta* **1970**, *4*, 347.

Scheme I

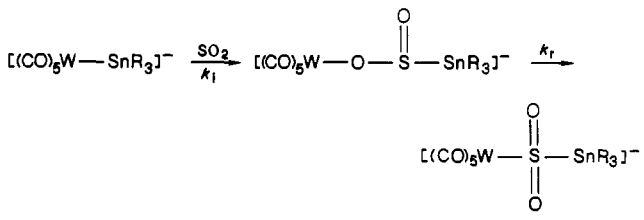

perature (−78 °C). Despite the unavoidable warming of solution that occurs during sampling, the infrared spectrum showed clean conversion of the stannyl complex to a species with carbonyl stretching frequencies of 1895 (sh), 1912 (s), and 2043 (w) cm^{-1}. When it was warmed to room temperature, this complex was observed to gradually convert to the sulfinate-*S* species, indicating that it is an intermediate in the SO_2 insertion process described above. Wojcicki and co-workers[21] have observed an isomerization from sulfinate-*O* to sulfinate-*S* in the reaction of some metal alkyls with SO_2 at low temperatures. The reaction of SO_2 with $[W(CO)_5Sn(CH_3)_3]^-$ is believed to proceed by an analogous mechanism (Scheme I). The sulfinate-*O* complex was found to be stable at 0 °C for several hours, during which time slow isomerization to the sulfinate-*S* compound occurred. This oxygen-bound intermediate is more stable toward isomerization than the alkyls studied by Wojcicki, which rearranged to the sulfinate-*S* compounds even at −18 °C.[21]

Proton and tin-119 NMR spectra also support the mechanism proposed in Scheme I. The resonance for the methyl protons of the trimethyltin group was found to shift from 0.17 ppm for $[PPN][W(CO)_5Sn(CH_3)_3]$ to 0.63 ppm for the intermediate that was trapped at −20 °C. After the solution was warmed to room temperature for 1 h, the resonance had shifted to 0.65 ppm ($J(^{117}Sn-CH_3)$ = 33.2 Hz; $J(^{119}Sn-CH_3)$ = 34.8 Hz; $(CD_3)_2CO$). The presence of a tin–proton coupling constant similar to that found in the starting material ($J(^{117}Sn-CH_3)$ = 35.5 Hz; $J(^{119}Sn-CH_3)$ = 37.0 Hz; CD_3CN)[9] demonstrates that the Sn–CH_3 bond is still intact and therefore is not cleaved by SO_2.

The $^{119}Sn\{^1H\}$ NMR was also examined for the SO_2 insertion reaction. $[PPN][W(CO)_5Sn(CH_3)_3]$ exhibited a resonance at −51.98 ppm (versus $SnMe_4$; $J(^{183}W-^{119}Sn)$ = 260.4 Hz; $(CD_3)_2CO$). After the addition of SO_2 to a cooled (−20 °C) THF solution of the trimethylstannyl complex, the spectrum failed to show a resonance that could be attributed to the intermediate. When the complex was warmed to room temperature, a signal appeared at −79.8 ppm, which is believed to be that of the sulfinate-*S* product.

The triphenyltin complex exhibited somewhat different behavior than the trimethyltin species. The infrared spectrum of $[PPN][W(CO)_5Sn(C_6H_5)_3]$ taken immediately after the addition of SO_2 showed no perceptible change. After 10 min the spectrum showed peaks that could be attributed to the starting material and the sulfinate-*O* and sulfinate-*S* complexes. After 30 min, complete conversion to the sulfinato-*S* complex was seen compared with the ca 10 min reaction time for $[W(CO)_5Sn(CH_3)_3]^-$. The presence of all three species in solution indicates a slower rate for the initial insertion process when compared with the rate of insertion for the trimethyltin analogue, where the starting material had undergone the SO_2 insertion step upon mixing. The rate constants for the rearrangement step can be assumed to be similar, i.e., $k_r(CH_3) \simeq k_r(C_6H_5)$, while the initial insertion rate constant is greater for R = CH_3 than for R = C_6H_5 ($k_i(CH_3) > k_i(C_6H_5)$). This ordering of reactivity is expected on the basis of the higher steric bulk of the phenyl groups.

The first reported instance of SO_2 insertion into a transition-metal–silicon bond has been found for the silyl complex $[PPN][W(CO)_5Si(CH_3)_3]$. Previous attempts of metal–silicon bond cleavage by SO_2 for $Mn(CO)_5Si(CH_3)_3$ and $(CH_3)_3SiFe(CO)_2(\eta\text{-}C_5H_5)$ were unsuccessful even under severe reaction conditions.[22] The high nucleophilicity of the anionic metal system apparently is sufficient to offset the usually unreactive metal–silicon bond. However, a very reactive substrate, SO_2, is necessary for insertion while the less electrophilic CO_2 failed to react. The reaction occurs at a much slower rate than for the stannyl analogue with insertion being complete only after ca. 2 h at room temperature and atmospheric pressure of SO_2 in THF solution. The product has carbonyl stretching frequencies similar to those found in the tin sulfinato-*S* complexes (1871 (m), 1935 (s), 2058 (w) cm^{-1}). The infrared spectrum of the solid in a mineral oil mull showed peaks at 1075, 1059, 1021, 1012, and 997 cm^{-1} in the S–O stretching region, indicating a sulfinato-*S* complex similar to that of the alkyl analogues.

Acknowledgment. The financial support of this research by the National Science Foundation (Grant CHE 86-03681) is greatly appreciated. The X-ray diffraction equipment was funded by a grant from the National Science Foundation.

Supplementary Material Available: A drawing with the labeling scheme for the $[PPN]^+$ cation in $[PPN][W(CO)_5Si(CH_3)_3]$ (Figure 1S), infrared spectra of the reaction products of $[PPN][W(CO)_5Sn(CH_3)_3]$ with SO_2 in the $\nu(CO)$ region in tetrahydrofuran (Figure 2S), a table of the crystallographic data (Table 1S), a table of anisotropic thermal parameters for $[PPN][W(CO)_5Si(CH_3)_3]$ (Table 2S), and a table of H atom coordinates and isotropic thermal parameters for $[PPN][W(CO)_5Si(CH_3)_3]$ (Table 3S) (6 pages); a listing of calculated and observed structure factor amplitudes for $[PPN][W(CO)_5Si(CH_3)_3]$ (Table 4S) (34 pages). Ordering information is given on any current masthead page.

(21) Jacobsen, S. E.; Reich-Rohrwig, O.; Wojcicki, A. *Inorg. Chem.* **1973**, *12*, 7.

(22) Bichler, R. E. J.; Clark, H. C. *J. Organomet. Chem.* **1969**, *23*, 427.